Image Cover Sheet

CLASSIFICATION	SYSTEM NUMBER
UNCLASSIFIED	513118

TITLE

A Preliminary Validation of the RANS Code TASCflow Against Model Scale Submarine Hydrodynamic Data

System Number:

Patron Number:

Requester:

Notes:

DSIS Use only:

Deliver to:

A Preliminary Validation of the RANS Code TASCflow Against Model Scale Submarine Hydrodynamic Data

George D. Watt
watt@drea.dnd.ca
Defence Research Establishment Atlantic

Kevin J. Knill
kevin@asc.on.ca
AEA Technology Engineering Software Ltd.

ABSTRACT

A preliminary evaluation of the RANS code CFX-TASCflow for predicting the hydrodynamic forces on a fully appended submarine at a Reynolds number of 20 million is described. Except for drag, TASCflow makes good predictions of the overall forces up to moderate incidence angles using wall functions with a 371,000 node grid. At high incidence angles the predictions break down due to inadequate modelling of separation and shed circulation. The predictions improve with a finer grid and different turbulence models. Drag predictions improve when the boundary layer is modelled in place of wall functions.

NOMENCLATURE

Standard submarine body fixed forces are used, with the origin located at the center of buoyancy.

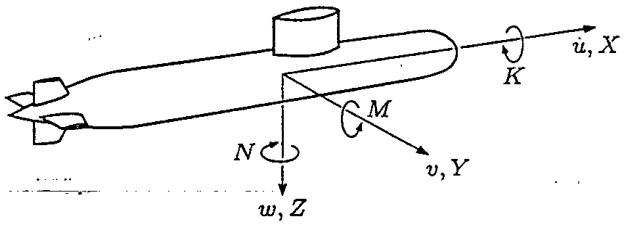

K, M, N	rolling, pitching, and yawing moments.
U	overall velocity: $\sqrt{u^2+v^2+w^2}$.
u, v, w	body axis velocities of vehicle.
X, Y, Z	axial, lateral, and normal forces.
β	angle of drift (yaw): $\tan^{-1}(-v/u)$.

1 INTRODUCTION

AEA Technology and DREA are evaluating the AEA Technology Reynolds Averaged Navier-Stokes (RANS) code CFX-TASCflow as a suitable tool for providing DREA with a robust underwater vehicle hydrodynamic force predictor. TASCflow is a second order, pressure/velocity coupled, finite element based control volume method that uses a body-fitted, non-orthogonal, structured grid and a multigrid solver. The code runs in single precision usually using a k-ϵ turbulence model and wall functions, but other turbulence models and a two-layer boundary layer model are also evaluated.

The objective of this work was to demonstrate how TASCflow would perform on underwater vehicle or model scale submarine problems using a grid sized for computations on a desktop workstation and built by someone with limited experience. The work was conducted in three phases over several years.

In the first phase, a masters student working with AEA Technology built a 371,000 node grid for a generic submarine configuration consisting of an axisymmetric hull with a sail and four symmetrical tailfins. TASCflow calculations using a k-ϵ turbulence model and wall functions were performed for the sub at yaw angles of 0, 10, 20, and 30 degrees at a Reynolds numbers of 20 million (based on hull length). These parameters correspond to the test parameters for experimental data that DREA and the Institute for Aerospace Research (IAR) obtained in the IAR 9 m wind tunnel in Ottawa [1]. This allowed the TASCflow predictions to be validated.

In the second phase, wall functions were again used. First, the grid nodal density in the outer flow was doubled and the calculations repeated. Second, the 371,000 node calculations at 30 degrees incidence, where agreement with experiment was poorest, were repeated with two k-ω turbulence models.

In the third phase, the phase 1 grid was expanded into the boundary layer and the phase 1 calculations repeated using a two-layer turbulence model and no wall functions. The k-ϵ model was used in the outer flow and standard one-equation and algebraic models were used to model k and the turbulence length scale ℓ in the boundary layer.

2 NUMERICS

2.1 The Grids

The phase 1 structured grid is shown in Figure 1. It is built from 32 blocks and contains 371,000 active

nodes. The dimensionless y^+ parameter values, viscous sublayer scaled measurements of the distance of the first layer of nodes off the submarine surface, varied from 1 to 1000 over the surface at the various incidence angles. The average y^+ value was 163 which falls within the recommended range of $30 < y^+ < 500$ for the wall functions.

The grid had a minimum skew angle of 20 degrees which is the minimum angle recommended for the TASCflow code.

TASCflow uses single precision floating point arithmetic to reduce memory requirements and accomodate large problems on desktop computers. However, this means that round-off error limits the cell aspect ratios a grid can have. This problem is alleviated by the use of wall functions which reduce the need for high grid densities near surfaces where the highest aspect ratio grid cells occur. The recommended maximum cell aspect ratio for TASCflow is 100:1. About 6% of the phase 1 grid aspect ratios were larger than this, with the largest being 780:1.

In phase 2, the phase 1 grid was built up to 932,000 nodes; wall functions were again used. The y^+ distribution was marginally improved and ranged from 6 to 860 with an overall average of 150. Aspect ratio and skew characteristics were unchanged.

In phase 3, the phase 1 grid was expanded into the boundary layer for a total of 835,000 active nodes. The boundary layer was modelled using a two-layer k-ϵ/k-ℓ model. The grid had an average of 3 nodes within a y^+ of 15, a maximum aspect ratio of 705:1, and a minimum skew angle of 15 degrees.

2.2 Boundary Conditions

All boundary conditions were steady state.

Either a conventional smooth wall, log-law wall function model or the two-layer k-ϵ/k-ℓ model were used on the surface of the vehicle.

Inflow velocity ($u = U\cos\beta$, $v = U\sin\beta$, $w = 0$), turbulence intensity (1%, to match the wind tunnel), and turbulence length scale (about half a hull diameter) were specified at the two upstream outer faces of the grid. When $\beta = 0$, this boundary condition was only applied to the single upstream face.

The two outflow faces (one when $\beta = 0$) had their average static pressure set to zero.

An 'opening' boundary condition was used on the remaining two faces (four when $\beta = 0$) in which the static pressure, turbulence intensity, and turbulence length scale were fixed at far field values. The flow direction was implicitly determined by the solution and could vary between inflow and outflow over a face.

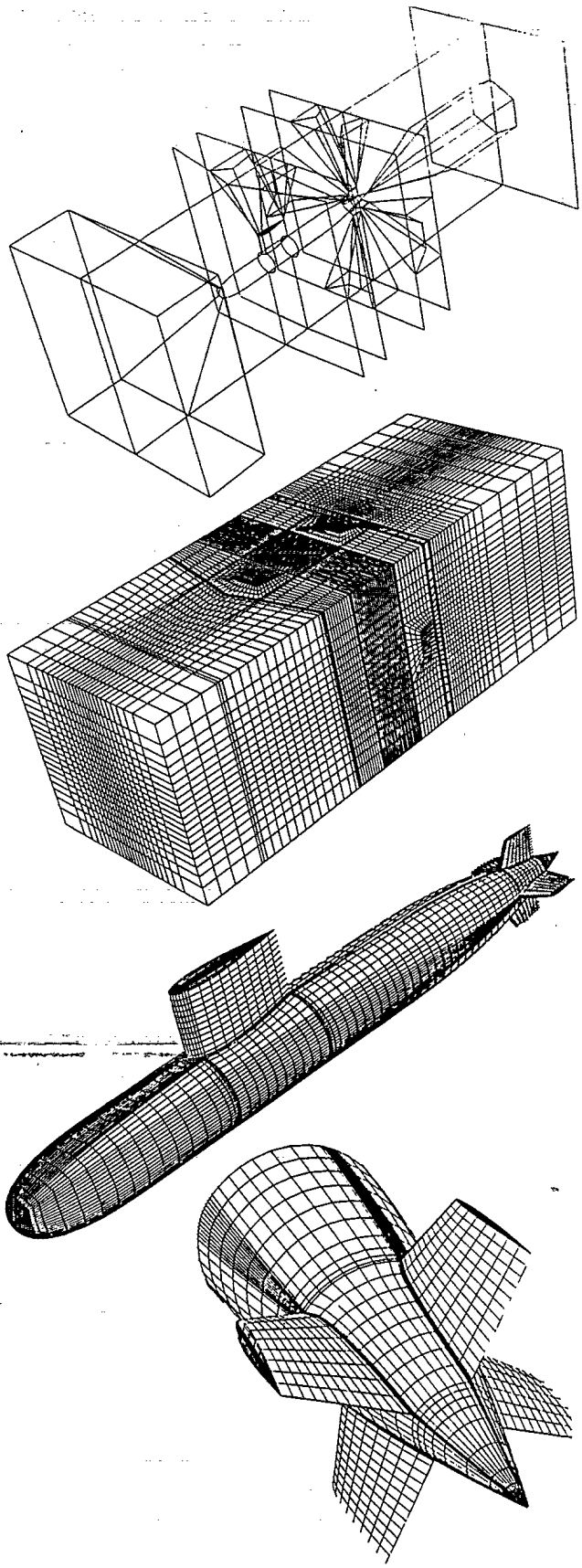

Figure 1 *The 371,000 node phase 1 grid.*

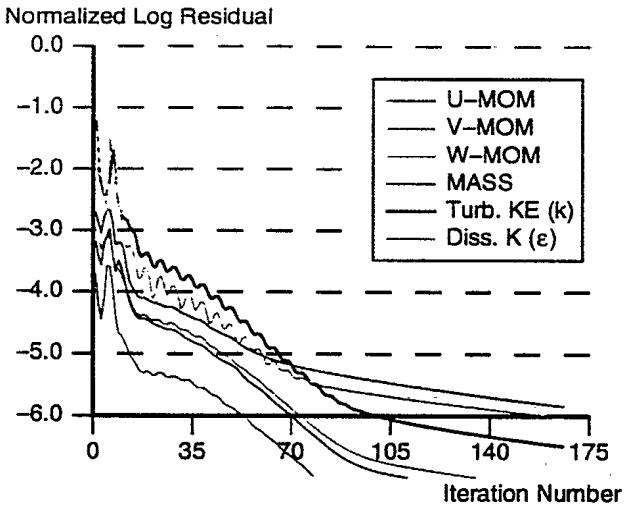

Figure 2 *Convergence history of RMS residuals for the 371,000 node grid, β = 20 degrees.*

For the phase 1 grid, a coalescence boundary condition was applied at the aft tip of the hull where the entire face of the trailing grid block degenerates to a point. This condition could not be used for the large grids as it prevented convergence. Solutions obtained without using the coalescence boundary condition had about a 10% variation in pressure over this degenerate face, creating a minor discontinuity in the solution at the aft tip of the hull. Perhaps finer longitudinal localized gridding here would solve this problem.

2.3 Convergence

In most cases the solutions converged satisfactorily, as shown in Figure 2. There were two exceptions. One was the coalescence boundary condition problem discussed above. The other occurred for the zero incidence calculations and was eventually traced to the multigrid solver; with the multigrid solver turned off, the zero incidence solutions readily converged.

3 RESULTS

The results were very good, as shown by the body axes force comparisons in Figure 3.* Except for axial force (negative drag), which is unimportant for vehicle stability and maneuvering performance predictions, all the forces were well predicted at low to moderate incidence angles. This range encompasses the standard towing tank test range (0 to 18 degrees) over which modern submarines are model tested before being built.

Of increasing importance to submarine safety are performance predictions for extreme maneuvers. This requires knowledge of the hydrodynamic forces at incidence angles larger than most towing tank facilities can handle, such as the 30 degree yaw angles obtained in the IAR 9 m wind tunnel. It is desirable to obtain this knowledge more economically, through the use of a CFD code. As Figure 3 shows, however, TASCflow is less accurate at predicting the forces at high yaw angles, especially the important out-of-plane forces (normal force and pitching moment) which directly influence depth-keeping. This is attributed to the inability of the code, grid, or turbulence model to correctly shed or transport circulation in vortices trailing from the sail and hull at large incidence angles.

Figure 4 shows experimental total pressure and transverse velocity fields in the propeller plane of the submarine, just aft of the tailplanes. The sail tip trailing vortex is clearly visible in the experimental plots two hull diameters away from the hull centerline at about 2 o'clock. The lower hull separation vortex is about one hull diameter away at 3 o'clock. This lower vortex contains the image circulation from the sail tip vortex which, at low incidence angles, remains bound in the hull afterbody. The out-of-plane forces are generated when this hull-bound circulation interacts with the crossflow along the afterbody (the Magnus effect). These forces roll-off at large yaw angles as the hull-bound circulation is shed in the lower body separation vortex.

Figure 4 shows that TASCflow is not modeling these trailing vortices well, which means the trailing sail circulation remains near, if not still bound in, the hull afterbody. Thus, TASCflow overpredicts the out-of-plane forces at high yaw angles.

The high incidence out-of-plane force predictions improve when 1) the turbulence model is replaced with either of two variations of the k-ω turbulence model and 2) the grid nodal density in the outer flow is increased. High incidence axial force predictions improve with these changes as well, but the two-layer model improves axial force over the full incidence range.

Figure 5 shows the TASCflow total pressure contours and transverse velocity vectors for the large grids. When the nodal density in the outer flow is increased (932,000 node grid) the total pressure better reflects experiment. However, the transverse velocity vectors show that circulation is still not adequately modelled. When the nodal density in the boundary layer is increased (835,000 node grid) there is no improvement in the pressure predictions.

* Proprietary considerations prevent publication of y-axis scales with these data.

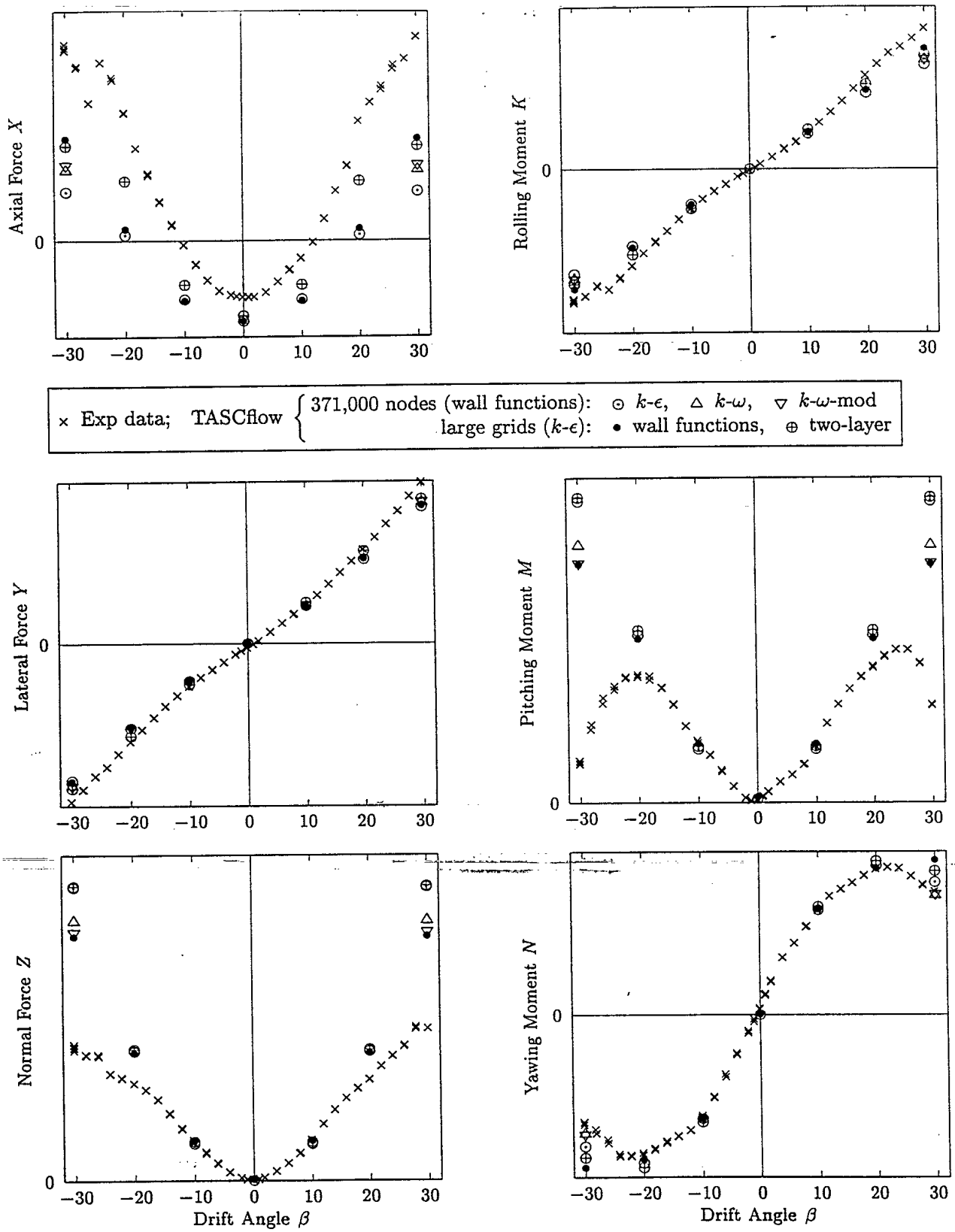

Figure 3 *Experimental data and TASCflow predictions for the submarine overall forces (**R** = 20 million). The 371,000 node calculations use wall functions. The large grid calculations (932,000 node grid using wall functions and 835,000 node grid using the two-layer model) use the k-ϵ turbulence model.*

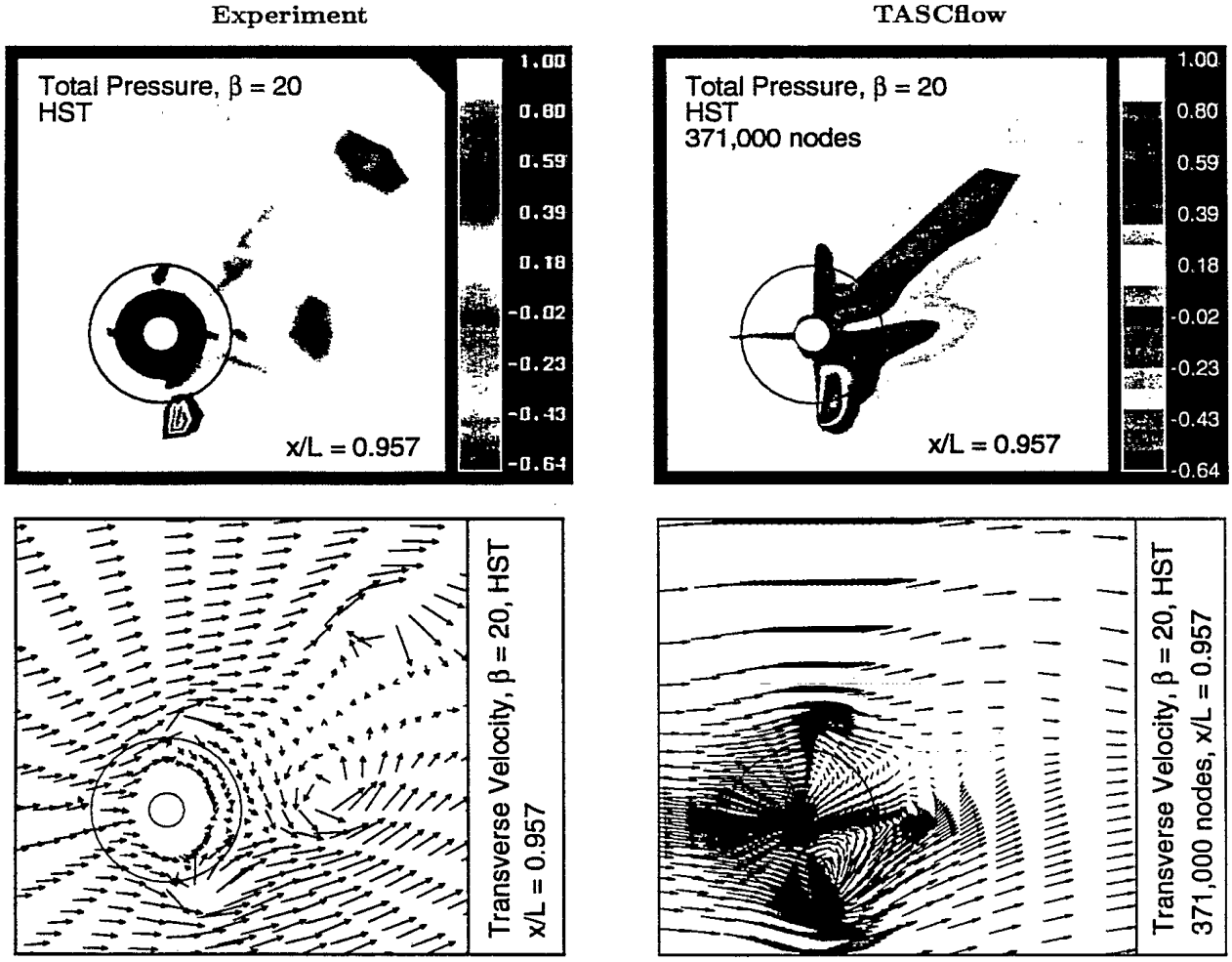

Figure 4 *Total pressure coefficient contours and transverse velocity vectors in the submarine propeller plane at $\beta = 20$ degrees. The white disc in the middle of each figure is the hull. The black annulus in the experimental plot is a flow region where data was not obtained. The large circles in the figures represent the maximum hull diameter. The velocity vector length's are proportional to the transverse velocity magnitudes.*

4 DISCUSSION

These results suggest that grid density in the outer flow should be increased and the turbulence model optimized to improve modelling of shed/trailing vorticity and of the out-of-plane forces. This is consistent with the findings of other submarine CFD researchers.

Zierke [2] found that about 10 nodes were needed in the core of a vortex to prevent numerical diffusion during convection. Figures 4 and 5 lack this resolution (velocity vector density equals nodal density in the figures), especially in the sail tip vortex.

The best turbulence model for submarine flows has yet to be determined. Early submarine CFD work [3] found that the standard algebraic Baldwin-Lomax model required modifications to adequately predict separation (wall-functions were not used). Subsequent work [4] used the k-ω two-equation model, but it was noted that k-ω overpredicts Reynolds stress in the outer boundary layer region.

AEA Technology recently carried out calculations with their unstructured CFX-TfC code using a 334,000 node version of the phase 1 grid and both k-ϵ and anisotropic Reynolds stress turbulence models. Wall functions were also used. The six-equation Reynolds stress model provided substantially better drag predictions than k-ϵ but only marginally improved out-of-plane force predictions.

Future work will address the above issues in more detail and extend the validation to other model configurations [2]. In addition, AEA Technology has recently provided DREA with an improved wall function formulation and a double precision version of the TASCflow code for evaluation.

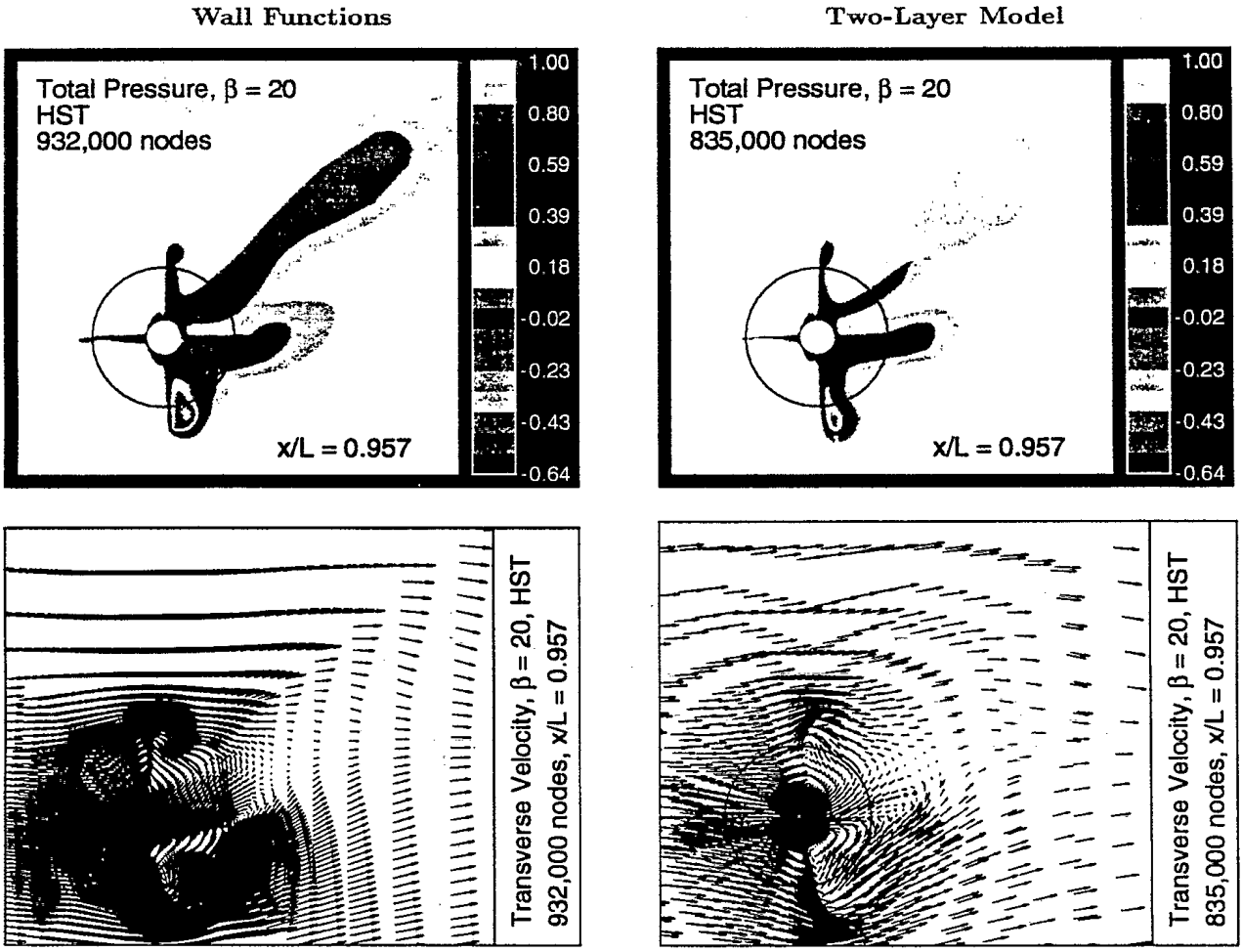

Figure 5 *TASCflow total pressure and transverse velocities from the $\beta = 20$ degree large grid predictions.*

5 CONCLUDING REMARKS

TASCflow does a good job of predicting the overall forces at low to moderate incidence angles, except for drag. This incidence range encompasses the test regime of conventional towing tank facilities. The authors know of no other non-experimental tool that can match this accuracy.

At high incidence angles, the current TASCflow overall force predictions break down due to inadequate modelling of separation and shed circulation. These predictions improve with a more optimum turbulence model and with finer gridding in the regions of separated flow.

TASCflow drag predictions improve when wall functions are replaced with a boundary layer calculation. However, drag characteristics are not critical to submarine maneuvering studies. In fact, the overall results of this work suggest that using wall functions may be an acceptable way to gain the memory necessary to adequately grid the trailing vortex fields in the outer flow of a maneuvering vehicle.

REFERENCES

1. Nguyen, V.D., Drolet, Y., and Watt, G.D., "Interference of Various Support Strut Configurations in Wind Tunnel Tests on a Model Submarine," AIAA 95–0443, 33rd Aerospace Sciences Meeting and Exhibit, Reno, January 1995.
2. Zierke, W.C. (editor), "A Physics-Based Means of Computing the Flow Around a Maneuvering Vehicle," Applied Research Laboratory, TR 97–002, January 1997.
3. Sung, C.H., Fu, T.C., Griggin, M.J., and Huang, T.T., "Validation of Incompressible Flow Computation of Forces and Moments on Axisymmetric Bodies at Incidence," AIAA 95–0528, AIAA 33rd Aerospace Sciences Meeting, Reno, January 1995.
4. Liu, C., Zheng, X., Liao, C., Sung, C.H., and Huang, T.T., "Preconditioned Multigrid Methods for Unsteady Incompressible Flows," AIAA–97–0445, 35th Aerospace Sciences Meeting, Reno, January 1997.

#513118